

ABS/PMMA 블렌드와 ABS/PMMA/MBS 블렌드의 특성: 고무입자 크기의 영향

Jin Ding^{***}, ZhenMing Yue^{*}, Jiao Sun^{*}, JiCui Zhou^{*}, and Jun Gao^{*†}

^{*}School of Mechanical, Electrical and Information Engineering, Shandong University

^{**}Department of Mechanical and Electrical Engineering, Weihai Vocational College

(2016년 1월 25일 접수, 2016년 4월 21일 수정, 2016년 5월 25일 채택)

Properties of ABS/PMMA Binary Blend and ABS/PMMA/MBS Ternary Blend: Influence of Rubber Particle Size

Jin Ding^{***}, ZhenMing Yue^{*}, Jiao Sun^{*}, JiCui Zhou^{*}, and Jun Gao^{*†}

^{*}School of Mechanical, Electrical and Information Engineering, Shandong University, Weihai 264209, China

^{**}Department of Mechanical and Electrical Engineering, Weihai Vocational College, Weihai 264210, China

(Received January 25, 2016; Revised April 21, 2016; Accepted May 25, 2016)

Abstract: An analysis was performed on the effects of rubber particle size on the mechanical and optical properties of the acrylonitrile-butadiene-styrene (ABS)/poly(methyl methacrylate) (PMMA) blend and the ABS/PMMA/methacrylate-butadiene-styrene (MBS) blend. This work found that when the particle size is 0.22-0.23 μm , the impact strength value of the ABS/PMMA blend is at its maximum and is the same as that of the ABS/PMMA/MBS blend. The optimum particle size is effective in toughening because it can trigger the shear yielding mechanism of the matrix. The miscibility and surface glossiness of the blends with 0.22 μm particle size were also much better than those of the blends with other particle sizes. This work provides new insights into the synergistic roles of rubber particle size and core-shell modifier in the toughening of ABS/PMMA blend with good impact toughness and high surface glossiness.

Keywords: rubber particle size, toughening, surface glossiness.

Introduction

In recent years, high impact Acrylonitrile-butadienestyrene (ABS) resin has attracted considerable research attention because of increasing environmental concerns and the esthetic appearance of its products.¹ The binary blend of ABS with poly(methyl methacrylate) (PMMA) shows great potential to replace polymerization-based high impact ABS because of its excellent surface glossiness, easy processability, and high mechanical strength.²⁻⁴ Nevertheless, despite the high preference for blends with good toughness in practical applications, the application of ABS/PMMA blend is far from widespread as expected because of the inherent brittleness exhibited by PMMA. Therefore, a great deal of effort has been exerted by both industry and academia to modify the properties of ABS/

PMMA blends.¹⁻¹⁰ Melt blending ABS/PMMA with some modifiers, such as ABS high-rubber powder⁶ and polycarbonate (PC),⁷ and nano-calcium modification,¹ such as organo-clays,⁸ provide economic but effective methods to enhance some properties of ABS/PMMA. Unfortunately, all the blending can not improve the toughness and surface glossiness simultaneously, which is not acceptable for various commercial applications.

Core-shell rubber modifiers, such as methacrylate-butadiene-styrene (MBS), are regularly used to improve the toughness of the polymer matrix because of two major attractive features: (1) the rubbery core provides resistance to impact, whereas the grafted glassy shell provides rigidity and miscibility with the polymer matrix; (2) after melt blending, the rubber particles retain the desired shape and dispersability.¹¹ Core-shell modifier has been widely used to toughen polymer materials, such as PMMA,¹² PC,¹³ and poly(vinyl chloride) (PVC).^{11,14-16} The different structures and morphologies of

[†]To whom correspondence should be addressed.

E-mail: shdgj@sdu.edu.cn

©2016 The Polymer Society of Korea. All rights reserved.

core-shell modifiers influence the impact resistance of the polymer matrix. Numerous studies on the mechanical behavior of rubber-toughened ABS/PMMA blend have been reported, yet reports on ABS/PMMA/MBS ternary blend are relatively few. We choose MBS as the modifier because of its sub-micron-sized core-shell particles, which can slightly improve the toughness of ABS/PMMA blend that impair surface glossiness.

The toughening improvement of polymers is attributed mainly to the presence of rubber particles that enhance the energy absorption capacity of the matrix, and the particle size of the impact modifier plays a decisive role in the toughening of polymers.¹⁷⁻²⁵ Generally, a suitable particle size is required to achieve an optimum toughening effect. Wu¹⁷ found that the optimum particle size was strongly dependent on the matrix properties. The tougher the matrix is, the smaller the optimum size. For example, the optimum particle sizes for toughening polystyrene, styrene-acrylonitrile (SAN), and PMMA are 2.5, 0.75±0.15, and 0.25±0.05 μm, respectively.²⁶ Importantly, Wu pointed out that bimodal size (i.e., distinctly large and small mixtures) rubber particles had a pronounced synergistic toughening effect in SAN. In this context, the interesting question arises as to whether the optimum rubber particle size varies with the ABS/PMMA binary blend, and whether the match between ABS/PMMA matrix rubber particle size and MBS modifier is synergistic to improve the toughening effect of the ABS/PMMA blend. Unfortunately, to our best knowledge, no effort has thus far been made to investigate the combined effects of core-shell modifier and optimum particle size for a given polymer matrix on improving toughness.

In the present work, an ABS/PMMA (80/20) blend was selected as the model blend and MBS (6 wt%) as the modifier. To decouple the effects of rubber particle size from those of interfacial adhesion, the rubber particle size was tailored by varying the screw rotation speed of the extruder (from 50 to 250 rpm) while maintaining the other processing conditions. Attention was focused on improving the mechanical and surface glossiness of the ABS/PMMA and ABS/PMMA/MBS blends with different rubber particle sizes, as well as on the toughening mechanisms responsible.

Experimental

Materials. All the materials used are commercially available. ABS copolymer (757 K) was obtained from Zhenjiang Chimei Chemical Co., Ltd., with the Vicat softening tem-

perature of 105 °C and the melt flow index of 1.8 g/10 min. PMMA (CM-211) with the melt flow index of 16 g/10 min and the Vicat softening temperature of 102 °C was obtained from Taiwan Chimei Chemical Co., Ltd. MBS (GR-6003) was provided by Dongguan AnChen Plastic Technology Co., Ltd., with the vicat softening temperature of 86 °C and the melt flow index of 5.5 g/10 min.

Sample Preparation. Prior to use, all the materials were dried at 80 °C for 12 h in an air-circulating oven. Melt blending ABS/PMMA and ABS/PMMA/MBS was prepared using a two-screw extruder (the screws had an L/D ratio of 40 and a diameter of 21.7 mm, SJSL-20, China) at 200-225 °C from hopper to die. To adjust the rubber particle size dispersed in the matrix, different screw rotation speeds of the extruder (50-250 rpm) were applied. After pelletizing, standard testing specimens were processed using a 68-ton injection molding machine (XL680, China). The injection temperature was set at 225-215 °C from the hopper to the nozzle, and the holding pressure was 50 MPa.

Measurements. Notched Izod Impact Testing: The notched Izod impact strength was evaluated using an impact tester (XC-5.5D, China) with a pendulum hammer of 2.75 J. Testing was carried out at room temperature (23 °C). The average value reported was obtained from at least five specimens.

Differential Scanning Calorimetry (DSC): Thermal analysis was performed on a SHIMADZU DSC-60 (Japan) under nitrogen atmosphere. For each measurement, about 10 mg of samples was placed into an aluminum. The temperature for the DSC thermal history was heated to 300 °C at 10 °C/min, which was maintained for 5 min, and then cooled to room temperature. The DSC curve was obtained by repeating the above operation and scanning the second heating process.

Scanning Electron Microscopy (SEM): The phase morphologies of the ABS/PMMA and ABS/PMMA/MBS blends were examined with an FEI Inspect field emission scanning electron microscope (FEI-NOVA NANOSEM 450) at an accelerating voltage of 5 kV. Samples for SEM observation were prepared using cryogenic nitrogen for about 90 min. To quantify the rubber particle sizes, an Image-Pro Plus software was used. For each specimen, at least 300 particles from different SEM micrographs were measured. The weight average particle size (D_w) was evaluated using the following eq:

$$D_w = \frac{\sum_{i=1}^k n_i d_i}{\sum_{i=1}^k n_i} \quad (1)$$

$$d_i = 2\sqrt{\text{Area}/\pi} \quad (2)$$

Where n_i is the number of rubber particles with the equivalent diameter of d_i .

The deformation mechanisms of the impact-fracture specimens were also characterized with FEI-NOVA NANOSEM 450 (Netherlands). The impact-fracture surface was obtained from the notched Izod impact testing, and the observations were focused on the regions of crack initiation. Prior to SEM characterizations, all the fracture surfaces were coated with a thin layer of gold.

Surface Glossiness: Surface glossiness was measured by a JFL-BZ60s (China) gloss meter. For the optical test, the average of five values was used in the analysis.

Results and Discussion

Effect of Rubber Particle Size on the Toughening of ABS/PMMA. To tailor the rubber particle size of the ABS dispersed phase in a wide range, the ABS/PMMA blend was prepared by extrusion under various screw rotation speeds (50–250 rpm). Figure 1 displays some representative SEM images of the blends. All the blends present a typical “sea-island” morphology with spherical rubber particles well dispersed in the ABS/PMMA matrix. Under the different screw rotation

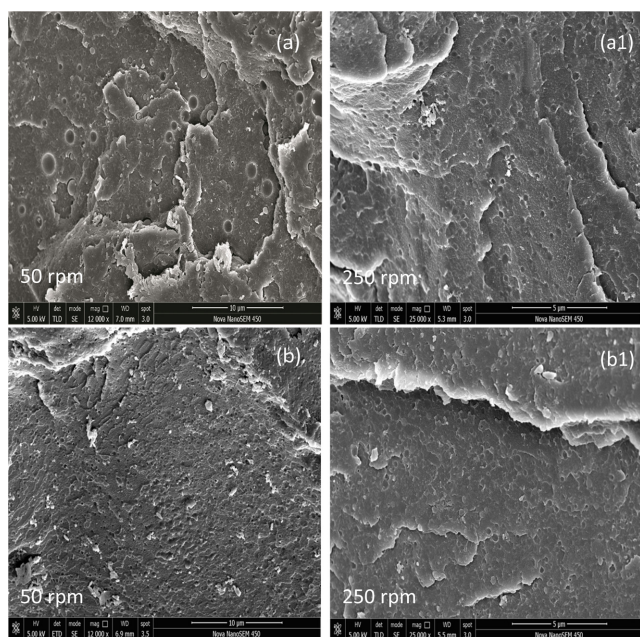


Figure 1. SEM images of cryogenically fracture surfaces (a) ABS/PMMA-50; (a1) ABS/PMMA-250; (b) ABS/PMMA/MBS-50; (b1) ABS/PMMA/MBS-250.

speeds, the average ABS/PMMA rubber particle size decreases significantly from 0.61 to 0.15 μm . The ABS/PMMA-50 blend shows the largest D_w , whereas the ABS/PMMA-250 blend shows the smallest D_w . Rubber particle size clearly decreases with increasing screw rotation speed because of the largely enhanced shear stress applied to the blend melts during extrusion. The lower the blend’s melt viscosity ratio, the better the droplet break-up and the lesser the coalescence. Similar results have been reported in literature.²⁷

The glass transition temperature (T_g) values from DSC scans reflect the miscibility of polymer blends. Generally a blend with single T_g value is termed as miscible blends. In the case of a totally immiscible blend system, the blend components retain their original T_g values that are independent of the blend composition. Partially miscible blends show two T_g values of the blend with respect to those of the pure polymers indicate the extent of component mixing.²⁸ If the difference of the T_g values of pure polymers is small ($<20^\circ\text{C}$), then overlapping of the transitions may occur as a single transition, so a single T_g is not efficient proof of the thermodynamic miscibility of the blend.²⁹ About T_g value of miscible blends, a number of theoretical equations have been proposed. In this study, we used the simple Fox equation to predict the T_g value of ABS/PMMA blend, which is given as

$$\frac{1}{T_g} = \frac{w_1}{T_{g1}} + \frac{w_2}{T_{g2}} \quad (3)$$

Where T_{g1} and T_{g2} are glass transition temperatures of constituent polymers, and w_1 and w_2 are their corresponding weight fractions. The theoretical T_g value of ABS/PMMA blend (80/20) is 99.65°C , and the experimental DSC curves are seen in Figure 2, and T_g values are obtained from the midpoint of the slope of the DSC thermograms and tabulated in Table 1. From Table 1, the T_g value is 99.72°C when the rubber particle size is 0.22 μm (ABS/PMMA-150), and this T_g value presents highest closeness to the theoretical T_g value, thereby confirming as miscible blends.

Figure 3 shows the notched Izod impact strength variation of all the prepared blends as a function of rubber particle size (D_w). The blend exhibits a rapid increase in impact toughness with the increase of rubber particle size from 0.1 to 0.22 μm . However, the toughness decreases rapidly from 0.22 to 0.6 μm , indicating that 0.22 μm is the optimum particle size for toughening ABS/PMMA. The result is in accordance with that of Wu, who reported that the optimum rubber particle size for toughening PMMA is $0.25\pm 0.05 \mu\text{m}$.²⁶ To obtain a clear

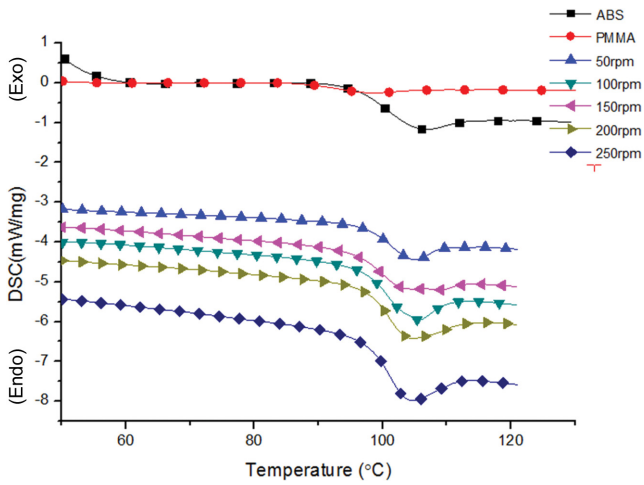


Figure 2. DSC thermograms for ABS, PMMA and ABS/PMMA blend with different screw rotation speed.

Table 1. T_g Values of ABS, PMMA and ABS/PMMA, ABS/PMMA/MBS Blends with Different Screw Rotation Speed

Samples	Particle size (μm)	T_g ($^{\circ}\text{C}$)
ABS	-	100.09
PMMA	-	97.92
ABS/PMMA-50	0.64	100.98
ABS/PMMA-100	0.35	100.43
ABS/PMMA-150	0.22	99.72
ABS/PMMA-200	0.178	100.70
ABS/PMMA-250	0.156	100.67
ABS/PMMA/MBS-50	0.243	100.99
ABS/PMMA/MBS-100	0.230	99.67
ABS/PMMA/MBS-150	0.213	99.89
ABS/PMMA/MBS-200	0.207	100.91
ABS/PMMA/MBS-250	0.169	100.98

understanding of how toughening depends on the rubber particle size, the impact-fracture surfaces of the blends with different rubber particle sizes were examined using SEM. For brevity, only the SEM images with a relatively large particle size (ABS/PMMA-50) and a relatively small particle size (ABS/PMMA-250) and a turning point of impact strength (ABS/PMMA-150) are presented in Figure 4. All the impact-fracture surfaces of the ABS/PMMA blend show many stress concentration points, and each of these points correspond to different sizes of yield bands [marked with a circle in Figures 4(a), (b), (c)] near the end of the drop hammer. The surfaces of all the samples exhibit large amounts of cavities resulting from

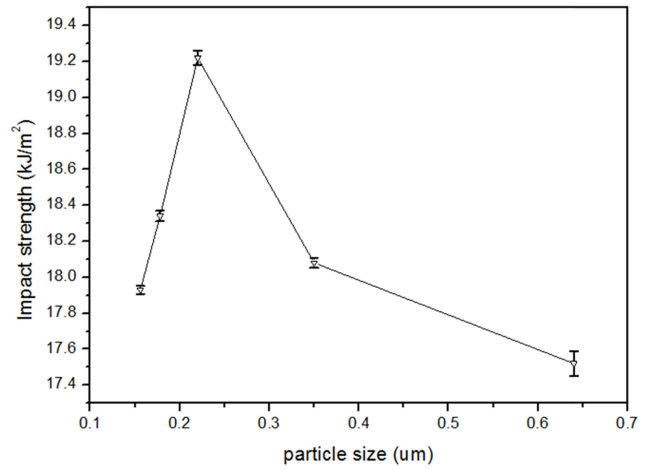


Figure 3. Notched Izod impact strength as a function of ABS/PMMA particle size (D_w).

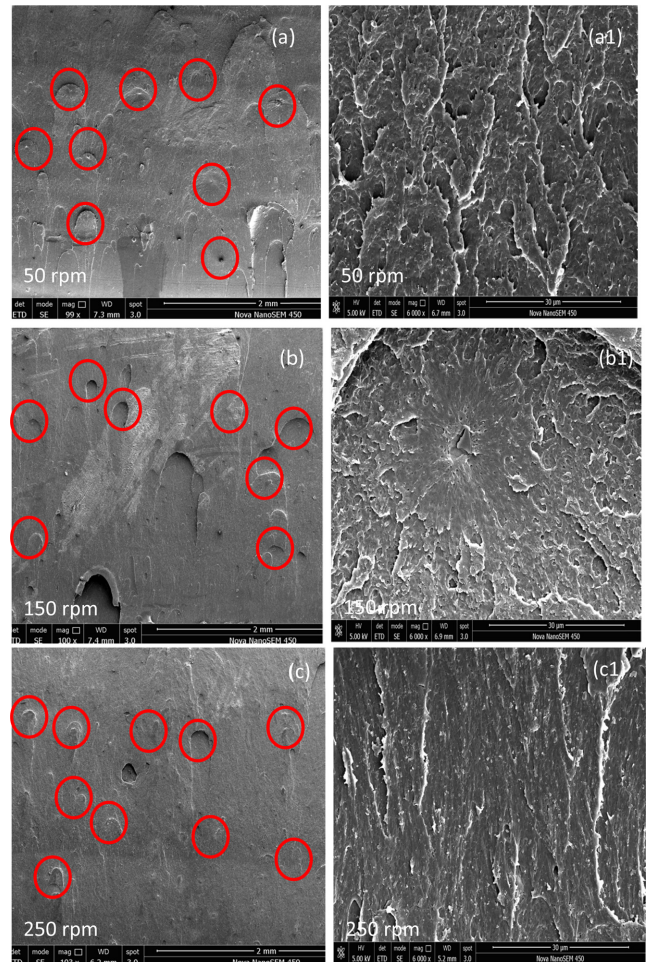


Figure 4. SEM images of impact fractured surfaces of (a) ABS/PMMA-50; (b) ABS/PMMA-150; (c) ABS/PMMA-250; (a1) ABS/PMMA-50, magnified 6000; (b1) ABS/PMMA-150, magnified 6000; (c1) ABS/PMMA-250, magnified 6000.

debonding between the rubber particles and the matrix, which exhibit appreciable plastic deformation and imply a typical ductile fracture characterized by rapid crack propagation. A comparison between the larger particle size [Figure 4(a1)] and the smaller one [Figure 4(c1)] indicates that the surface of small particles is smoother than that of the large particles. Therefore, we deduce that large rubber particles are much more effective in triggering pervasive multiple crazing of the amorphous matrix necessary for impact energy dissipation compared to relatively small ones. Numerous investigators have identified that only rubber particles with sizes larger than the critical values can effectively initiate crazing of the matrix around the particles.¹⁷ Dompas *et al.*³⁰ stated that if the rubber particle size is decreased below the critical value of ~ 200 nm, the impact toughness of the blend will substantially decrease and approach the value of the unmodified matrix. Our data on the rubber particle size of ABS/PMMA are in accordance with this, and $0.22 \mu\text{m}$ is found to be the turning point of impact strength. Bucknall *et al.*³¹ introduced a new model and successfully explained the observed relationships between particle size and impact behavior. They pointed out that maximum toughness is achieved when the rubber particles are large enough to cavitate a long way ahead of a notch or crack tip, but not so large that they initiate unstable crazes, and thus reduce fracture resistance. Thus, in our study, when the rubber particle size of ABS/PMMA is beyond $0.2 \mu\text{m}$, the impact strength value decreases.

Effect of Rubber Particle Size on the Toughening of ABS/PMMA/MBS. The core-shell modifier, MBS, plays an important role in the toughening of the ABS/PMMA blend.³² Our previous experiment results have verified it, as seen in Figure 5. From the results we can see that the Izod impact strength increases when the content of MBS below 6 wt%, but it decreases when increasing the content of MBS. However, whether an optimum rubber particle size exists for toughening ABS/PMMA/MBS is unclear as in the case for ABS/PMMA. With the aim of resolving this question, 6 wt% MBS was adopted as modifier for melt blending with ABS/PMMA under various extruder screw rotation speeds, ranging from 50 to 250 rpm, to tailor the rubber particle size in the blends. The result shows that the average rubber particle size (D_w) is smaller than that of the ABS/PMMA blend, as seen in Figure 1, and the D_w ranges from 0.167 to $0.243 \mu\text{m}$. This finding means a pronounced synergistic effect of ABS/PMMA/MBS occurs on toughening.

The reason for this effect is attributed to MBS not only act-

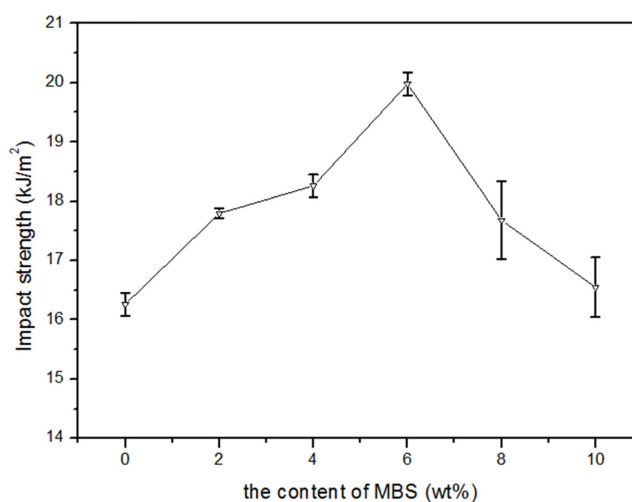


Figure 5. Notched Izod impact strength of ABS/PMMA/MBS blend as a function of the content of MBS (wt%).

ing as a modifier, but also as a compatibilizer. The core of MBS is polybutadiene copolymerized with styrene, which has the effect of toughening thermoplastic, and the shell of MBS is grafted PMMA, which has good miscibility with PMMA. As mentioned in the introduction, after melt blending, MBS can retain the desired shape, dispersability, and good dimensional stability. Hence, the rubber particle size of ABS/PMMA/MBS ternary blend only changes slightly with different screw rotation speeds.

Fortelny *et al.*³³ introduced a theoretical description of steady droplet size in polymer blends containing a compatibilizer. The equation is given as follows:

$$R = R_c + \frac{4\sigma_e}{\pi\eta_m f} \Phi \quad (4)$$

where R is the radius of the dispersed droplet, R_c is the critical radius, σ_e is the interface tension, η_m is the viscosity of the matrix, f is the function of rheological properties, and Φ is the volume fraction of the dispersed phase. The basic conclusion of the theory is that the addition of a compatibilizer leads to a decrease in R , so the average rubber particle size of ABS/PMMA/MBS blend is smaller than that of ABS/PMMA blend. Figure 6 and Table 1 give the T_g values of ABS/PMMA/MBS, and the results show that ABS/PMMA/MBS-100 and ABS/PMMA/MBS-150 are miscible systems.

Figure 7 shows the notched Izod impact toughness of ABS/PMMA/MBS blend with different rubber particle sizes. Note that the impact strength values change slightly, not as the results of the ABS/PMMA blend. However, the average

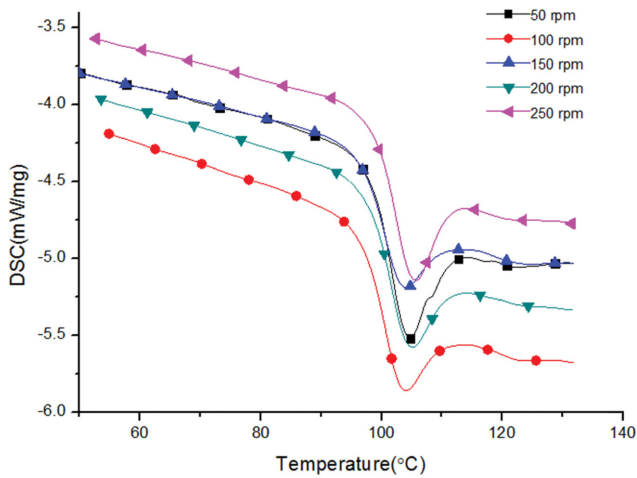


Figure 6. DSC thermograms for ABS/PMMA/MBS blend with different screw rotation speed.

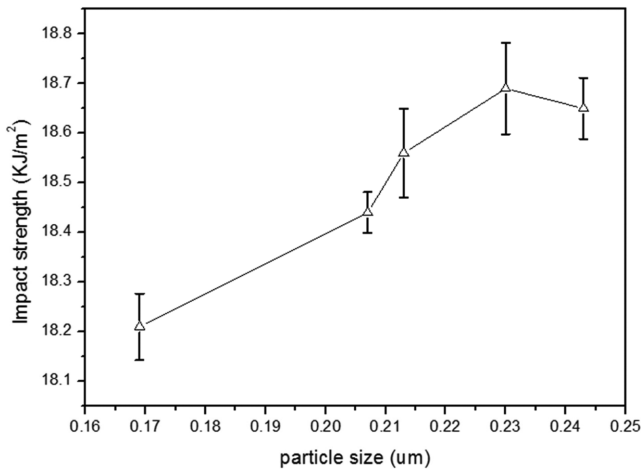


Figure 7. Notched Izod impact strength as a function of ABS/PMMA/MBS particle size (D_w).

impact strength value is higher than that of the ABS/PMMA blend. Figure 8 gives detailed information about the fracture surface of ABS/PMMA/MBS. All the impact-fracture surfaces of ABS/PMMA/MBS blend also show many stress concentration points, and each of these points correspond to different sizes of yield bands [marked with a circle in Figures 8(a) and (b)] near the end of the drop hammer. However, the numbers of yield bands are more than those of the ABS/PMMA blends, and the impact-fracture surfaces are coarser than those of the ABS/PMMA blends.

Surface Glossiness. For multiphase polymer materials, surface glossiness is normally limited by the presence of haziness or reduced clarity, which arises primarily from the failure to match the refraction indices of the polymer phases and par-

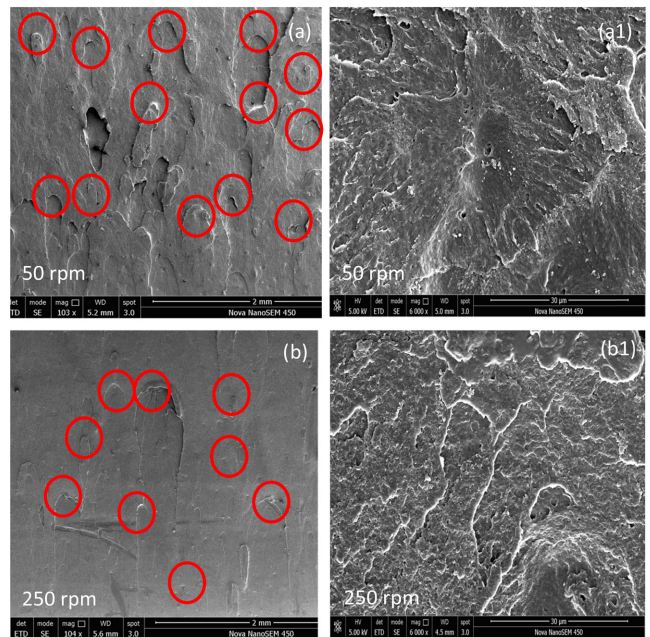


Figure 8. SEM images of impact fractured surfaces of (a) ABS/PMMA/MBS-50; (a1) ABS/PMMA/MBS-50, magnified 6000; (b) ABS/PMMA/MBS-250; (b1) ABS/PMMA/MBS-250, magnified 6000.

tle sizes perfectly.¹² Matching the refractive index of rubber with that of the ABS/PMMA blend is difficult because rubbers have relatively low refractive indices. Refractive index can be calculated using the Gladstone–Dale relation as follows:

$$\text{Refractive index (RI)} = \sum_{i=1}^k n_i v_i \quad (5)$$

Where n_i and v_i are the refractive index and volume fraction of the components. According to this relation, all blends designed to have the same composition in our work will have the same refractive index.

Figure 9 shows the relationships between rubber particle size and surface glossiness of the ABS/PMMA and ABS/PMMA/MBS blends. In Figure 9(a), the surface glossiness exhibits a linear decrease with the increase of rubber particle size. The maximum surface glossiness is 72.38 GS when the particle size is 0.156 μm (ABS/PMMA-250), because the smaller the rubber particle size, the lower the haziness value and the higher the light transmission. In Figure 9(b), surface glossiness initially increases from 0.169 to 0.213 μm , and then decreases. The particle size of 0.213 μm (ABS/PMMA/MBS-150) is the turning point. With increasing the rotation speed, the shear rate is largely increased, and the rubber particles are dispersed evenly, so the transmission of the samples is improved. How-

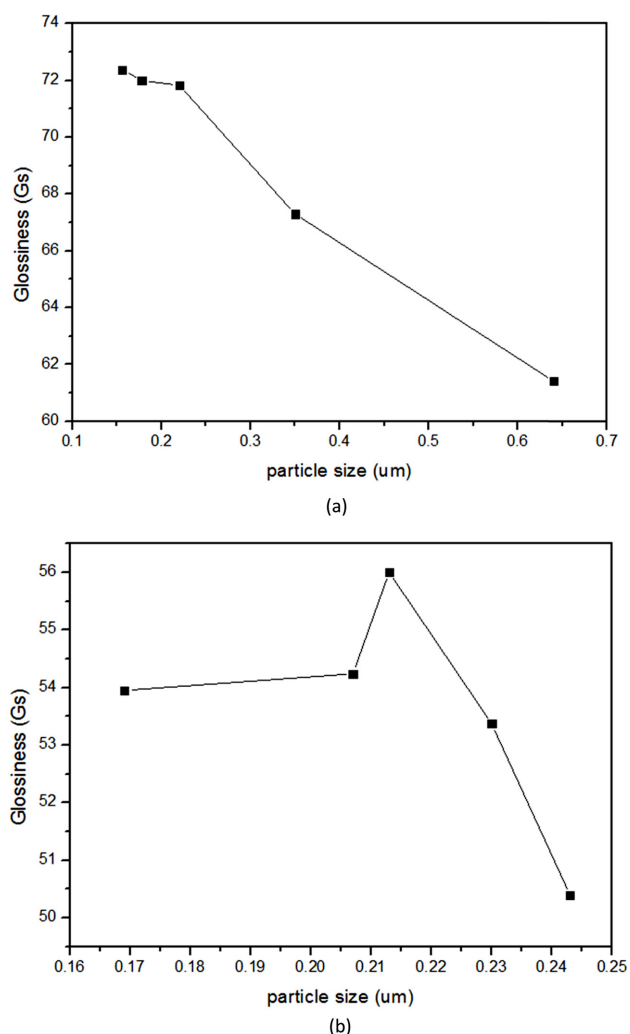


Figure 9. Surface glossiness as a function of particle size (D_w): (a) ABS/PMMA blend; (b) ABS/PMMA/MBS blend.

ever, the rubber phase concentration in ABS/PMMA/MBS ternary blend is higher than that of in ABS/PMMA binary blend. With increasing the shear rate, the number of larger size rubber particles is decrease, more and more small particles appear (especially D_w below 0.2 μm). The small size particles reinforce the backward scattering, which will reduce the transmission.³⁴ However, the average surface glossiness of the ABS/PMMA/MBS ternary blend is worse than that of the ABS/PMMA binary blend. The reason for this outcome is that the rubber core in MBS does not match the refractive index of the matrix phases and has poor light transmission.

Conclusions

The influence of rubber particle size on the properties of the

ABS/PMMA and ABS/PMMA/MBS blends was investigated and discussed in this work. Our experimental results demonstrate that effective toughening is achieved when the particle size is approximately 0.22 μm for the ABS/PMMA blend. Large rubber particles are much more effective in triggering pervasive multiple crazing of the amorphous matrix necessary for impact energy dissipation compared to relatively small ones, but not so large that they initiate unstable crazes and thus reduce fracture resistance. For ABS/PMMA/MBS blend, the particle size and impact strength values vary slightly, exhibiting the synergistic toughening effect. When the particle size is approximately 0.21-0.23 μm , all the blends can obtain good miscibility and good surface glossiness. This work can provide a general guideline for the toughening of ABS/PMMA blends with good surface glossiness.

Acknowledgements: The work was supported by the National Science and Technology Support Project (Grant No.2011BAF16B01) and Weihai city Science and Technology Plan Project (Grant No.2015GGX030).

References

1. A. M. Zhang, G. Q. Zhao, Y. J. Guan, and G. W. Chen, *Polym. Compos.*, **31**, 1593 (2010).
2. A. M. Zhang, G. Q. Zhao, and Y. J. Guan, *J. Appl. Polym. Sci.*, **132**, 1 (2015).
3. B. K. Kim, C. H. Choi, and X. M. Xie, *J. Polym. Sci., Part B: Polym. Phys.*, **35**, 829 (1996).
4. S. H. Wang, J. Gao, S. X. Lin, P. Zhang, J. Huang, and L. L. Xu, *Mater. Sci. Eng.*, **62**, 1 (2014).
5. B. K. Kim, L. K. Yoon, and X. M. Xie, *J. Appl. Polym. Sci.*, **66**, 1531 (1997).
6. A. M. Zhang, G. Q. Zhao, J. Gao, and Y. J. Guan, *Polym. Plast. Technol. Eng.*, **49**, 296 (2010).
7. J. Rybnicek, R. Lach, W. Grellmann, M. Lapcikova, M. Slouf, K. Zdenek, Z. Krulis, E. Anisimov, and J. Hajek, *Polym.*, **57**, 87 (2012).
8. N. Tayebe, G. Hamid, and A. Anmad, *J. Appl. Polym. Sci.*, **126**, 1637 (2012).
9. S. H. Wang, J. Gao, S. X. Lin, P. Zhang, and J. Huang, *Appl. Mech. Mater.*, **496-500**, 322 (2014).
10. S. H. Wang, J. Gao, S. X. Lin, P. Zhang, and J. Huang, *Appl. Mech. Mater.*, **496-500**, 327 (2014).
11. C. Zhou, H. Liu, M. Chen, G. Wu, and H. Zhang, *Polym. Eng. Sci.*, **52**, 2523 (2012).
12. L. Ren, M. Y. Zhang, Y. R. Wang, H. Na, and H. X. Zhang, *Polym. Adv. Technol.*, **25**, 273 (2014).
13. S. Sun, Y. He, X. Wang, and D. Wu, *J. Appl. Polym. Sci.*, **116**, 2451 (2010).

14. M. Chen, S. Wang, C. Zhou, Z. Liu, and H. Zhang, *Polym. Plast. Technol. Eng.*, **52**, 814 (2013).
15. Y. Fan, H. L. Zhang, and G. F. Wu, *Polym. Korea*, **39**, 852 (2015).
16. G. F. Wu, H. L. Zhang, and H. X. Zhang, *Polym. Korea*, **39**, 809 (2015).
17. S. Wu, *Polym. Eng. Sci.*, **26**, 1855 (1985).
18. R. A. Pearson and A. F. Yee, *J. Mater. Sci.*, **26**, 3828 (1991).
19. C. B. Bucknall, A. Karpodinis, and X. C. Zhang, *J. Mater. Sci.*, **29**, 3377 (1994).
20. O. K. Muratoglu, A. S. Argon, and R. E. Cohen, *Polym.*, **36**, 921 (1995).
21. D. S. Ayre and C. B. Bucknall, *Polym.*, **39**, 4785 (1998).
22. G. M. Yang and D. J. Chung, *Polym. Korea*, **27**, 493 (2003).
23. H. G. Jeoung, D. W. Chung, and K. H. Ahn, *Polym. Korea*, **25**, 744 (2001).
24. S. Y. Fu, X. Q. Feng, B. Lauke, and Y. W. Mai, *Compos Part B: Eng.*, **39**, 933 (2008).
25. B. Lauke, *Compos. Sci. Technol.*, **68**, 3365 (2008).
26. S. Wu, *Polym. Eng. Sci.*, **30**, 753 (1990).
27. H. T. Oyama, *Polym.*, **50**, 747 (2009).
28. Z. K. Marwat and M. K. Baloch, *Eur. Polym. J.*, **66**, 520 (2015).
29. G. N. Kumaraswamy, C. Ranganathaiah, M. V. DeepaUrs, and H. B. Ravikumar, *Eur. Polym.*, **42**, 2655 (2006).
30. D. Dompas and G. Groeninckx, *Polym.*, **35**, 4743 (1994).
31. C. B. Bucknall and D. R. Paul, *Polym.*, **50**, 5539 (2009).
32. S. H. Jin, U.S. Patent 0,281,603 (2013).
33. I. Fortelny and A. Zivny, *Polym.*, **41**, 6865 (2000).
34. Y. Ping, X. Ying, L. Xiao, Z. R. Zhao, and S. Y. Guo, *Polym. Mater. Sci. Eng.*, **31**, 50 (2015).